

ARTICLE

Specific interaction of Smn, the spinal muscular atrophy determining gene product, with hnRNP-R and gry-rbp/hnRNP-Q: a role for Smn in RNA processing in motor axons?

Wilfried Rossoll, Ann-Kathrin Kröning, Uta-Maria Ohndorf¹, Clemens Steegborn¹, Sibylle Jablonka and Michael Sendtner*

Institut für Klinische Neurobiologie, Department of Neurology, University of Würzburg, Josef-Schneider Strasse 11, D-97080 Würzburg, Germany and ¹Max-Planck-Institut für Biochemie, Abteilung Strukturforchung, Am Klopferspitz 18a, D-82152 Planegg-Martinsried, Germany

Received October 2, 2001; Revised and Accepted November 1, 2001

Spinal muscular atrophy (SMA), the most common hereditary motor neuron disease in children and young adults is caused by mutations in the telomeric *survival motor neuron (SMN1)* gene. The human genome, in contrast to mouse, contains a second *SMN* gene (*SMN2*) which codes for a gene product which is alternatively spliced at the C-terminus, but also gives rise to low levels of full-length SMN protein. The reason why reduced levels of the ubiquitously expressed SMN protein lead to specific motor neuron degeneration without affecting other cell types is still not understood. Using yeast two-hybrid techniques, we identified hnRNP-R and the highly related gry-rbp/hnRNP-Q as novel SMN interaction partners. These proteins have previously been identified in the context of RNA processing, in particular mRNA editing, transport and splicing. hnRNP-R and gry-rbp/hnRNP-Q interact with wild-type Smn but not with truncated or mutant Smn forms identified in SMA. Both proteins are widely expressed and developmentally regulated with expression peaking at E19 in mouse spinal cord. hnRNP-R binds RNA through its RNA recognition motif domains. Interestingly, hnRNP-R is predominantly located in axons of motor neurons and co-localizes with Smn in this cellular compartment. Thus, this finding could provide a key to understand a motor neuron-specific Smn function in SMA.

INTRODUCTION

Spinal muscular atrophy (SMA) is an autosomal recessive disorder characterized by muscle weakness and atrophy (1) which is caused by progressive motor neuron degeneration (2). The gene defect underlying SMA has been identified as homozygous mutations or deletion of the *survival motor neuron (SMN1)* gene (3). The *SMN* gene is duplicated on human chromosome 5q13, and the second copy (termed *SMN2*) is also expressed (3,4). Although the two copies differ in only 5 bp, full-length protein is predominantly produced from *SMN1*. Most of the *SMN2* transcripts undergo alternative splicing of exon 7, which results in the preferential expression of C-terminally truncated SMN protein (3,5–8). At the cellular level, reduced expression of full-length SMN leads to apoptotic cell death of motor neurons in the anterior horn of the spinal

cord and consequently to SMA (9). Similarly, motor neuron degeneration is observed in mouse models in which Smn levels are reduced (10), exon 7 is deleted (11) or human *SMN2* is expressed at low levels (12,13) on an *Smn* null background (14).

The full-length *SMN* gene product consists of 294 amino acids. It is found in the cytoplasm and in the nucleus. Within the nucleus it appears concentrated in specific structures called gems (for gemini of coiled bodies) (15). SMN is a tudor domain protein that is part of at least one large multiprotein complex which includes the Smn interacting protein 1 (Sip1/Gemin2) (15–18), the putative DEAD-box helicase dp103/Gemin3 (19,17), the dp103/Gemin3 interacting protein Gemin4/GIP1 (18,20), profilins (21) and spliceosomal U snRNP proteins of the Smith antigen (Sm) class (7,15,16,20,22).

*To whom correspondence should be addressed. Tel: +49 931 201 5767; Fax: +49 931 201 2697; Email: sendtner@mail.uni-wuerzburg.de

The authors wish it to be known that, in their opinion, the first two authors should be regarded as joint First Authors

Present addresses:

Clemens Steegborn, Department of Chemistry, The Scripps Research Institute, 10550 North Torrey Pines Road, La Jolla, CA 92037, USA

Uta-Maria Ohndorf, Laboratory of Molecular Neurobiology and Biophysics, The Rockefeller University, 1230 York Avenue, New York, NY 10021, USA

Moreover, SMN interacts with U snRNAs in the cytoplasm of *Xenopus laevis* oocytes (16).

The association with U snRNAs and Sm proteins points to a role for SMN in the biogenesis and function of spliceosomal U snRNPs (16,22,23). Following oligomerization, the U snRNPs are imported into the nucleus, where they function in pre-mRNA splicing (16). In addition, the nuclear pool of SMN contributes to nuclear pre-mRNA splicing (8,20,24). Another tudor domain protein, SMNrp is a pre-mRNA splicing factor required for the formation of the mature spliceosome in *Xenopus laevis* oocytes (20). However, the role of SMN in snRNP assembly, regeneration and in RNA splicing appears essential for all cell types and does not explain the specificity of SMA for motor neurons. Thus, additional functions appear at least as relevant in the context of the disease.

The helicase RHA which binds RNA polymerase II was identified in complexes with SMN (24). In addition, the snRNP proteins fibrillarin and GAR1 were described as direct binding partners of the SMN protein (25,26). Like SmB, Smd1, Smd3, LSm4 and RHA (24,27), they contain a RG-rich domain that is necessary for SMN interaction (25). Recently, a new gene defect causing spinal muscular atrophy with respiratory distress (SMARD1) was discovered as immunoglobulin μ -binding protein 2 (IGHMBP2), a protein which is a member of the DEAD-box family of RNA helicases (28). IGHMBP2 resembles Gemin3 and SMN by co-localization with the RNA-processing machinery in the cytoplasm and the nucleus. These findings underline the connection between SMA, helicase function and RNA metabolism.

SMN may also exert additional functions beyond RNA metabolism. Evidence comes from the observation, that the papillomavirus nuclear transcription activator E2 interacts with SMN *in vitro* (29). SMN enhances E2-dependent transcriptional activation of reporter genes (29). In addition, the SMN interaction partner dp103/Gemin3 has originally been identified as a factor that interacts with viral and cellular transcription factors (30).

There is no evidence so far that splicing of mRNA is disrupted in motor neurons of SMA patients. Splicing of candidate mRNAs appears unaffected in motor neurons of mouse models exhibiting symptoms of SMA (10). In homozygous coilin knock-out mice, coiled bodies fail to recruit Smn and Sm snRNPs in gems, but the mice do not develop any neuromuscular disorder (31). Thus, despite recent progress in the understanding of the function of SMN in pre-mRNA splicing, very little is known about the cause of the motor neuron-specific pathology in SMA. Here, we describe two novel highly related SMN interaction partners, hnRNP-R (heterogenous nuclear ribonucleoprotein) and gry-rbp, which has previously been found as a glycine-arginine-tyrosine-rich RNA-binding protein. Gry-rbp has been identified as component of the spliceosome complex (32). An alternatively spliced version of this protein, which was named NASP1 (NS1-associated protein 1) (33) or SYNCRIP (synaptotagmin-binding, cytoplasmic RNA-interacting protein) (34), have been found as a component of the apobec-1 editosome (35). Recently, gry-rbp has been identified as an SMN-binding protein and was renamed hnRNP-Q (36).

By co-immunoprecipitation, we observed that both hnRNP-R and hnRNP-Q bind wild-type Smn but not truncated or mutated Smn. Both hnRNP gene products are ubiquitously

expressed. In spinal cord, expression of both proteins is developmentally regulated with highest levels at embryonic day (E)19. hnRNP-R protein is mainly expressed in motor axons and to a much lower degree in sensory axons. Our findings that Smn interacts with hnRNP-R and hnRNP-Q and co-localizes with Smn in axons of motor neurons may help to understand a putative motor neuron-specific function of Smn, for example, in axonal transport or editing. Thus, our observations could contribute to elucidate the specific pathophysiological events leading to SMA.

RESULTS

SMN interacts with hnRNP-R and hnRNP-Q

In order to identify specific binding partners of the Smn protein we employed a yeast two-hybrid (Y2H) screen using a mouse brain library. Among the identified potential Smn interaction partners two clones containing the C-terminal portion of highly related proteins were found. These clones correspond to genes which belong to the class of *hnRNPs*, *hnRNP-R* and *hnRNP-Q*. Homologous sequences have been described previously as human *hnRNP-R* (37) and murine *gry-rbp* (GenBank accession no. AF093821). We obtained the full cDNA sequence of both genes by RT-PCR from mouse brain RNA. The 5' end sequence of murine *hnRNP-R* was obtained by RACE techniques. Mouse hnRNP-R and hnRNP-Q share 82% identity and 90% similarity on the protein level (Fig. 1). Both amino acid sequences are 98–99% identical to their human orthologues. A relatively acidic auxiliary N-terminal region is followed by two well defined and one degenerated RNA recognition motifs (RRMs). The C-terminal part contains an RGG motif. Both proteins show high similarity to the apobec-1 interacting proteins ACF and ABBP-1 (35). The identified clones contain coding regions spanning amino acids 469–632 (hnRNP-R) and amino acids 323–623 (hnRNP-Q), including the C-terminal RGG domains.

hnRNP-R and hnRNP-Q interact with wild-type Smn but not with inactive mutants

In order to characterize the cellular role of both hnRNP-R and hnRNP-Q, polyclonal antibodies against the divergent N-terminal peptides of both proteins were raised in rabbits (Fig. 1). In western blots of mouse spinal cord and other tissue extracts, both antisera detect proteins of the expected molecular size. Specific binding can be blocked by pre-adsorption of the antiserum with the corresponding peptides used for immunization (Fig. 3A and B). To prove that hnRNP-R and hnRNP-Q indeed interact with Smn, co-immunoprecipitation was employed. HEK 293 cells were transiently transfected with the cDNAs encoding *hnRNP-R*, *hnRNP-Q*, murine *Smn* and GFP as a negative control. Cell lysates were subjected to immunoprecipitation with both peptide antisera. Western blot analysis detected Smn only in immunoprecipitates from *Smn* transfected cells. The interaction of Smn and hnRNP-R and hnRNP-Q was also seen in the absence of hnRNP-R overexpression, indicating that Smn also binds to endogenous hnRNP-R and hnRNP-Q in HEK 293 cells (Fig. 2A). We then investigated whether mutated Smn isoforms corresponding to SMA-specific SMN mutants are able to interact with hnRNP-R

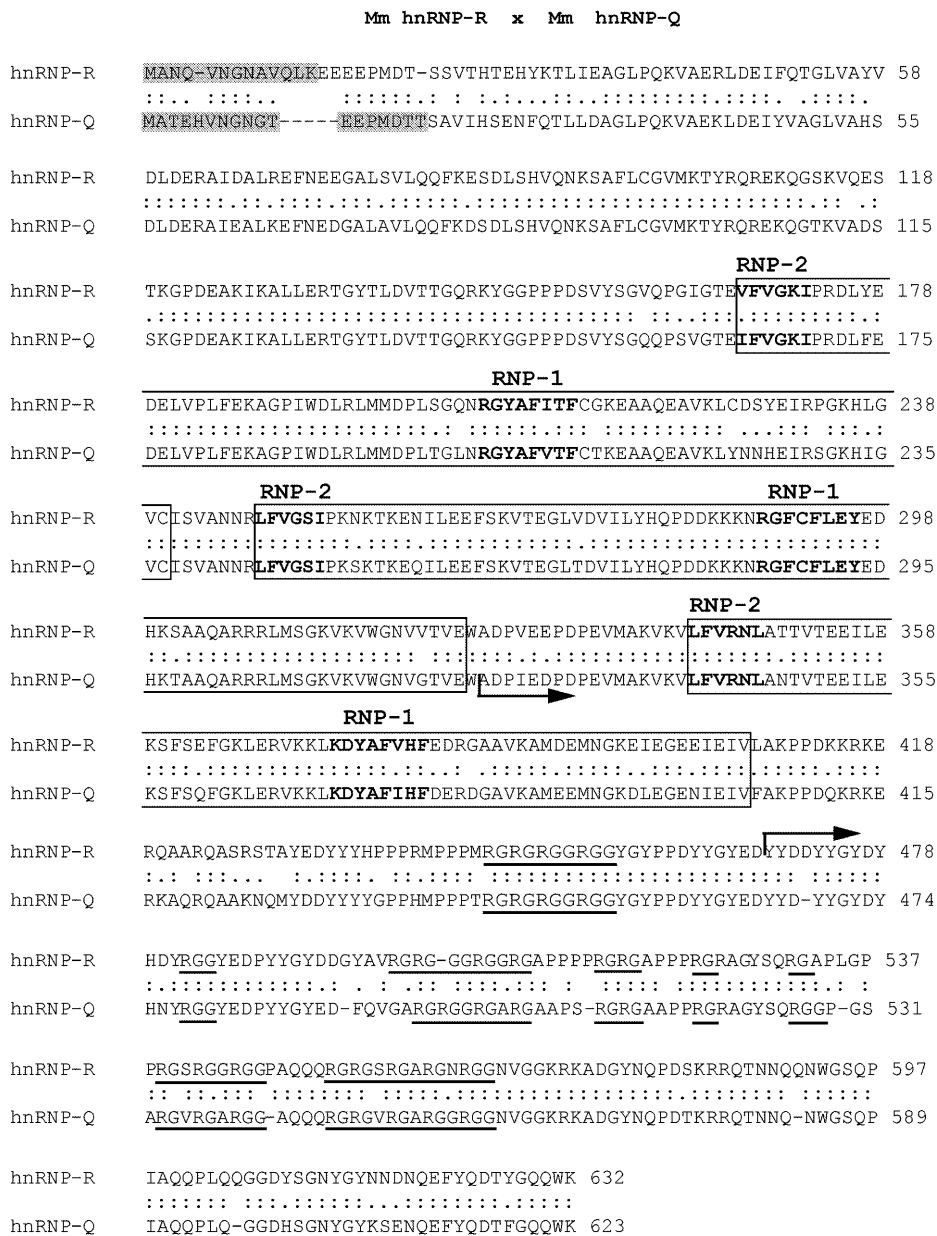


Figure 1. Sequence alignment of murine hnRNP-R and hnRNP-Q. The amino acid sequences of hnRNP-R and hnRNP-Q are aligned. The peptides used for immunization of rabbits are indicated in grey. RRM s are marked by boxes. RNA-binding RNP-1 and RNP-2 signatures are marked in bold. Arrows indicate the clones isolated in the Y2H screen. The repetitive sequences of the RGG domain are underlined.

and hnRNP-Q. HEK 293 cells were transfected transiently with the cDNAs for murine *Smn* and mutated murine *Smn* isoforms carrying a FLAG epitope corresponding to human mutations E134K, S262I, T274I, Y272C, G279V, Δexon7, Δexon5, Δexon5 and 7 (3,38–43). In order to increase the sensitivity for detection of weak interactions we also over-expressed hnRNP-R or hnRNP-Q. Western blot analysis of the protein extracts using an antibody against FLAG was applied as a control for comparable expression levels of the mutated *Smn* isoforms (Fig. 2C). Cell lysates were used for immunoprecipitation with both antisera. Western blot analysis detected *Smn* only in immunoprecipitates of cell lysates transfected

with wild-type *Smn*. Our results indicate that both hnRNP-R proteins do not interact with mutant *Smn* (Fig. 2B).

hnRNP-R and hnRNP-Q are widely expressed and developmentally regulated in mouse spinal cord

The expression of both genes was tested by western blot analysis of extracts from various neural and non-neural tissues from adult mouse. hnRNP-R was detected at highest levels in brain and at low levels in spinal cord, heart, lung, liver and spleen. hnRNP-Q was found in all tissues tested. Highest levels were observed in lung, liver and brain, and low levels in kidney and muscle (Fig. 3A). Thus, both hnRNP-R

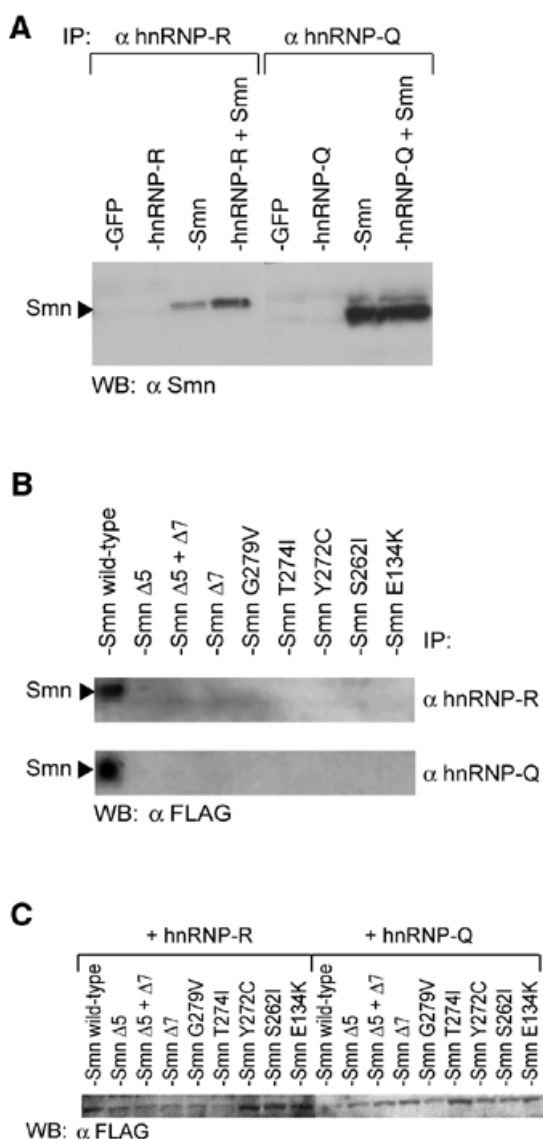


Figure 2. Snn interacts with hnRNP-R and hnRNP-Q *in vivo*. (A) Co-immunoprecipitation of Snn with polyclonal antibodies for hnRNP-R and hnRNP-Q. Cell lysates were prepared from HEK 293 cells transiently transfected with expression plasmids for hnRNP-R, hnRNP-Q, Snn and GFP (negative control) as indicated. Snn was co-precipitated with hnRNP-R and hnRNP-Q. Relatively high levels of Snn could also be precipitated with antibodies against hnRNP-R and hnRNP-Q in the absence of hnRNP-R overexpression, due to the relatively high endogenous levels of these proteins in HEK 293 cells (C). (B and C) Co-immunoprecipitation of mutated Snn proteins with polyclonal antibodies for hnRNP-R and hnRNP-Q. Lysates of transfected HEK 293 cells were used for co-immunoprecipitation. Cells were transfected with *hnRNP-Q* or *hnRNP-R* and *Snn* or one of the mutated *Snn* forms found in SMA patients. All Snn proteins were FLAG tagged. The precipitate was used for western blot analysis (B). Immunoprecipitations were carried out with polyclonal hnRNP-R antibodies. Detection of co-precipitated Snn or mutated isoforms was performed with monoclonal anti-FLAG antibody. Mutated Snn isoforms could not be co-precipitated with hnRNP-R or hnRNP-Q (C). The cells lysates were checked for expression of the mutated SMN protein by western blot with monoclonal anti-FLAG antibody.

and hnRNP-Q resemble Snn by their widespread distribution.

We also compared hnRNP-R and hnRNP-Q protein levels in spinal cord at various developmental stages. Spinal cords were

isolated from mice at embryonal day 14, 19, post-natal day 2, 15 and from 12-month-old mice. Tissue lysates were probed with both antisera. Both proteins appear developmentally regulated with highest expression levels during late embryogenesis and a steep decline after birth (Fig. 3B). To test whether these changes are due to transcriptional or post-transcriptional mechanisms, we performed RT-PCR using RNA from various tissues and spinal cord from different developmental stages. Primers corresponding to the coding region of *hnRNP-R* and *hnRNP-Q* genes were used (Fig. 3C). The results confirm that these genes are ubiquitously expressed. However, RNA levels for *hnRNP-R* and *hnRNP-Q* appeared similar in the developing and post-natal spinal cord. This indicates that the reduced levels of hnRNP-R and hnRNP-Q are caused by post-transcriptional and/or post-translational mechanisms. It is possible that interaction with Snn which is also reduced at the protein level in the post-natal spinal cord is necessary for the stability of hnRNP-R and hnRNP-Q, as previously described for SIP1/Gemin2 (44,45).

hnRNP-R protein is located in the axons of motor neurons

In order to study the functional relationship between Snn and the hnRNP-R and hnRNP-Q proteins in more detail we investigated the localization of both proteins in spinal motor neurons *in situ* and in cell culture. Unfortunately, the hnRNP-Q antiserum produced significant background staining in tissue sections even after pre-adsorption with the corresponding peptide and therefore could not be used for this study. Spinal cord sections of adult mice were double-stained with anti-hnRNP-R peptide antiserum and anti-Snn antibodies. Specific hnRNP-R staining of the motor neurons was observed in specific structures within the nucleus, the cytoplasm and neurites (Fig. 4A and B). Co-localization with Snn was detectable in the cytoplasm and neuronal processes. In contrast to Snn, which appeared concentrated to gem-like structures in the nucleus, hnRNP-R did not stain these nuclear structures (Fig. 4D–F).

In order to define whether hnRNP-R is more concentrated in axons or dendrites of motor neurons, we stained cultured embryonic motor neurons. Motor neurons were purified from mouse embryos (E14) and cultured for 7 days. Fixed cells were incubated with anti-hnRNP-R antiserum and monoclonal anti-Snn antibodies (Fig. 4G–I) and as a control with pre-adsorbed hnRNP-R antiserum (Fig. 4C). These experiments confirmed the results of cellular staining obtained *in vivo* with spinal cord sections. Interestingly, one neurite appeared stronger labelled by the anti-hnRNP-R antiserum in the cultured motor neurons. To address whether the staining was specific for axons, we performed co-staining with an axon-specific marker, the phospho-tau-1 (clone PC1C6) monoclonal antibody. This experiment shows that hnRNP-R is predominantly concentrated in axons but not in dendrites (Fig. 4J–L).

To verify the axonal localization of hnRNP-R *in vivo*, cross-sections of the sciatic nerve were stained with anti-hnRNP-R antiserum and monoclonal anti-Snn antibodies. Strong hnRNP-R-specific staining was detected in the axons, but not in Schwann cells (Fig. 5A–L). We also performed immuno-staining of other subgroups of nerves (Fig. 5M–T) including the facial and phrenic nerves (Fig. 5N, R and M, Q) which almost exclusively contain motor fibres, and the perineal nerve (Fig. 5P and T), a predominantly sensory nerve.

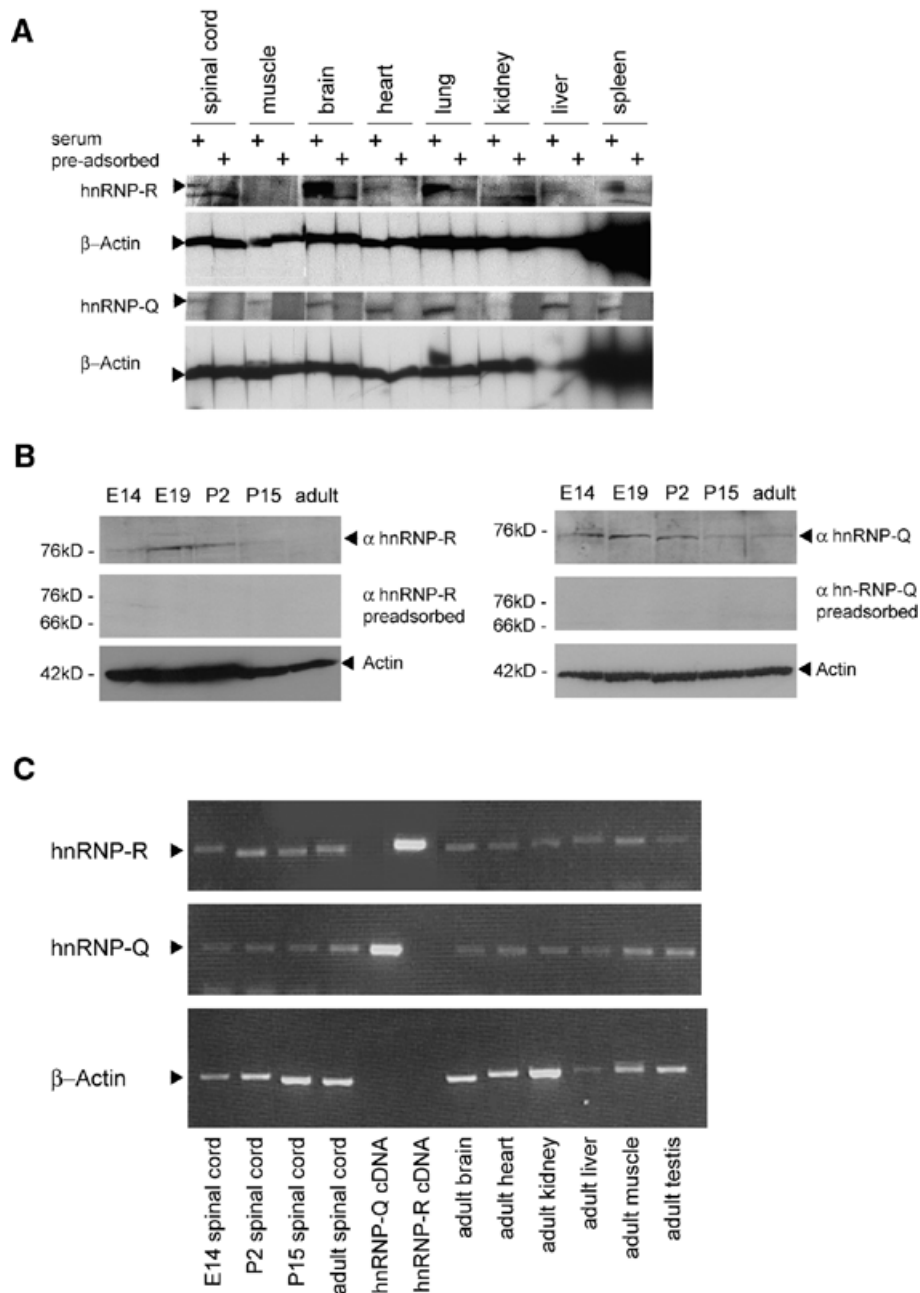


Figure 3. Tissue distribution and developmental regulation of hnRNP-R and hnRNP-Q RNA and protein. **(A)** Western blot analysis of hnRNP-R and hnRNP-Q protein in various tissues of adult mice. Tissue lysates were electrophoresed, blotted and probed with anti-hnRNP-R and anti-hnRNP-R-Q antisera. Equal protein content in the individual lanes was verified by stripping and reprobing with β -actin antibody. As a specificity control for hnRNP-R and hnRNP-Q under those conditions, blots were probed with pre-adsorbed polyclonal antibodies. **(B)** Western blot analysis of hnRNP-R and hnRNP-Q protein content in embryonic and post-natal mouse spinal cord. The polyclonal antibodies detect single bands (82 kDa for hnRNP-R, 74 kDa for hnRNP-Q). Negative controls were performed by probing additional blots with pre-adsorbed polyclonal antibodies. Equal protein content in the individual lanes was controlled by stripping off the first antibody and reprobing with β -actin antibody (42 kDa, bottom). Strongest hnRNP-R and hnRNP-Q signals were detectable at E19 and P2. The relative signal intensity became lower between post-natal days 2 and 15; lowest levels were found in adult, 12-month-old mice. **(C)** RT-PCR analysis of hnRNP-R and hnRNP-Q RNA in various tissues. hnRNP-R and hnRNP-Q cDNA clones (100 fg each) were used as internal control for the specificity of the PCR reaction, and RT-PCR with β -actin primers was performed as control for comparable RNA levels added to the PCR reactions.

Strong staining was detectable in the phrenic and facial nerve. Only a few fibres were stained in the sensory perineal nerve.

This suggests that hnRNP-R is predominantly present in the axons of motor neurons.

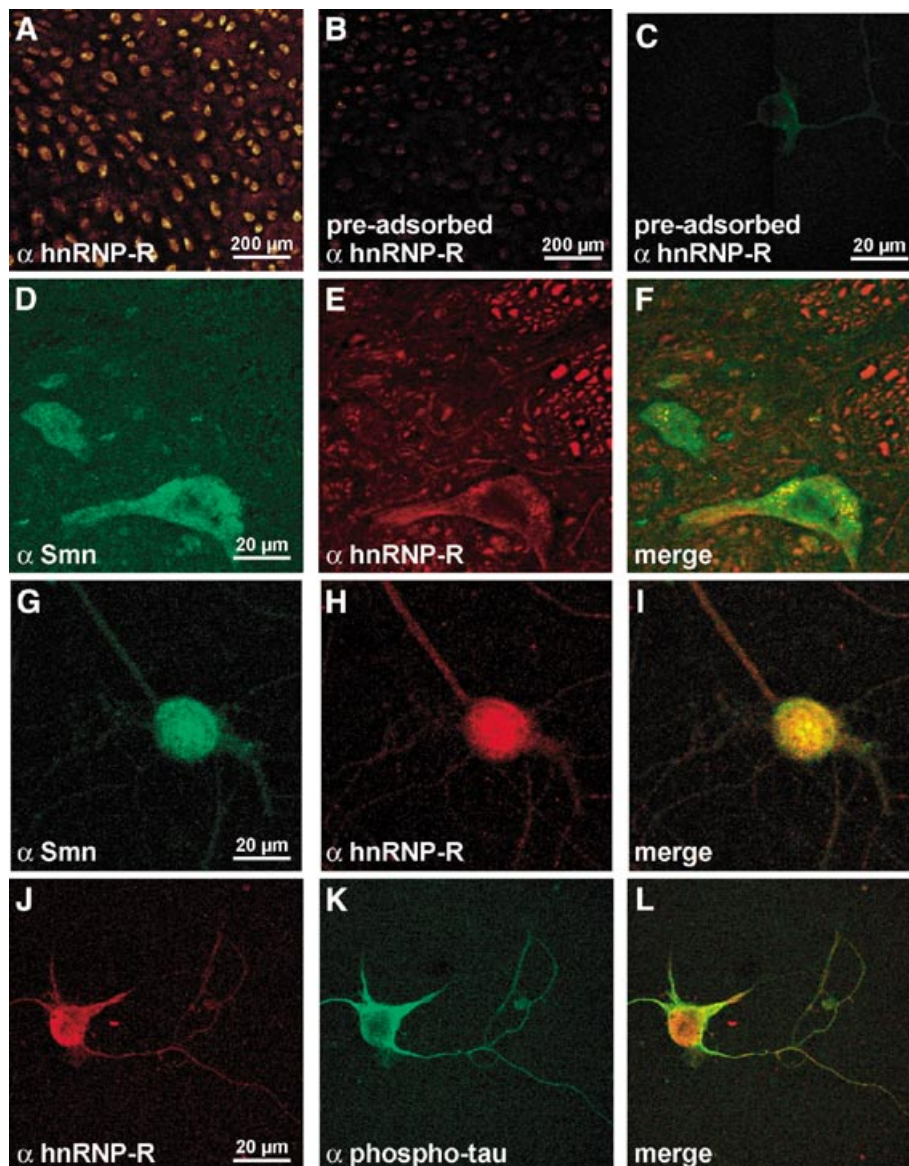


Figure 4. Subcellular distribution of hnRNP-R in motor neurons. (A) Distribution of hnRNP-R and Smn in the cell body of mouse spinal motor neurons. hnRNP-R was detectable in spinal motor neurons in the adult mouse spinal cord. (B) Pre-adsorption control with the corresponding hnRNP-R peptide of spinal cord sections. (C) Pre-adsorption control for motor neuron culture. At higher magnification, Smn was detectable in gem-like structures within the nucleus, in the cytoplasm and neurites. hnRNP-R was not enriched in gem-like structures. (D) Staining with a monoclonal SMN antibody, (E) staining with polyclonal hnRNP-R antibody, (F) a merge of (D) and (E). (G–L) Subcellular distribution of hnRNP-R in cultured embryonic motor neurons. (G) SMN was detectable in gem-like structures within the nucleus and cytoplasm and in neurites of cultured embryonic mouse motor neurons. hnRNP-R was found in the nucleus (no enrichment in gems), in the cytoplasm and in one neurite. (H) Staining with hnRNP-R antibodies, (I) a merge of (G) and (H) [pre-absorption control for specificity of the hnRNP-R staining is shown in (C)]. (J–L) Co-localization of hnRNP-R and the axonal marker PC1C6 anti-phospho-tau. (K) hnRNP-R staining of a cultured spinal motor neuron after 7 days in culture. (J) Phospho-tau was detectable in the cytoplasm and in the axon. (L) A merge of (J) and (K).

hnRNP-R binds single-stranded RNA

hnRNP-R and truncated hnRNP-R isoforms lacking a small N-terminal part (hnRNP-R Δ N; amino acids 26–632), the C-terminal RGG domain (hnRNP-R Δ C; amino acids 1–433), or both (hnRNP-R $\Delta\Delta$; amino acids 26–433), were cloned into *Escherichia coli* expression plasmids. Deletion of the C-terminal RGG domain turned out to be essential for expression in *E. coli* (data not shown). hnRNP-R $\Delta\Delta$ and hnRNP-R Δ C could be purified to homogeneity by using anion exchange and two

affinity chromatography steps. Analytical gel filtration on Superose-12 indicated that hnRNP-R $\Delta\Delta$ is monomeric in solution (data not shown). Electrophoretic mobility shift analysis showed that hnRNP-R $\Delta\Delta$ binds single-stranded RNA (Fig. 6A). Testing three different RNA oligonucleotides revealed that hnRNP-R $\Delta\Delta$ preferentially binds poly(U) in comparison to poly(A) RNA, and that oligonucleotides with six uridine residues are bound with higher affinity than oligonucleotides with four uridine nucleotides. Furthermore, analytical

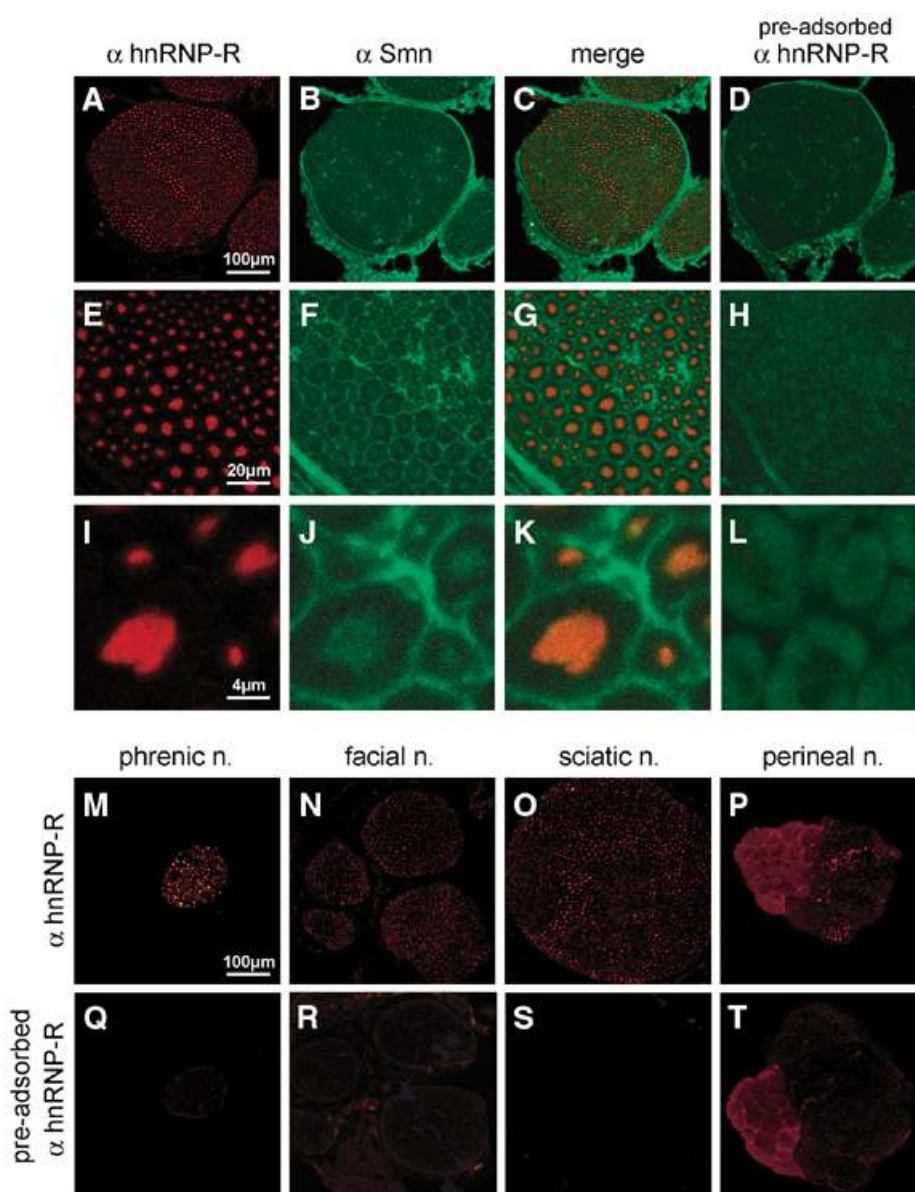


Figure 5. Subcellular distribution of hnRNP-R in motor and sensory nerves of the adult mouse. Transverse sections of the sciatic nerve were double stained against hnRNP-R (A, E and I) and Smn (B, F and J). hnRNP-R was detectable in the axons. Smn immunoreactivity was found at low levels in axons and in surrounding cells. Corresponding merges (C, G and K) and specificity controls with preadsorption for hnRNP-R staining (D, H and L) are shown to the right. (M–P) Cross-sections of the phrenic nerve (M), the facial nerve (N), the sciatic nerve (O) and the sensory perineal nerve (P). All sections were processed and stained in parallel in the same experiment. (Q–T) Corresponding controls in which the hnRNP-R antiserum was pre-adsorbed with specific peptide. Strong staining was detected in predominant motor nerves (phrenic and facial nerves), only subgroups of fibres appeared strongly stained in the sciatic nerve whereas staining in the sensory perineal nerve was very weak.

gel filtration on Superose-12 showed that the poly(U) oligonucleotide induced the formation of an hnRNP-R $\Delta\Delta$ homo-oligomer, most probably a dimeric form (data not shown).

Resistance to proteases was investigated in the absence or presence of equimolar amounts of synthetic RNA. After limited proteolysis, the resulting fragments were separated by gel electrophoresis and sequenced (Fig. 6B). Both proteinase K and subtilisin digestion resulted in relative protection of a fragment spanning amino acids 117–325 which contains the two N-terminal RRM motifs. This protection is enhanced in

the presence of RNA. Thus, these two RRM domains appear as primary binding sites for RNA (Fig. 6C). Taken together, these results confirm a potential function of hnRNP-R as an RNA-binding protein.

DISCUSSION

Previous genetic studies have provided strong evidence that mutations or deletions in the *SMN1* gene are the primary cause of SMA. However, it remains unclear why systemically reduced levels of functional Smn protein lead to specific

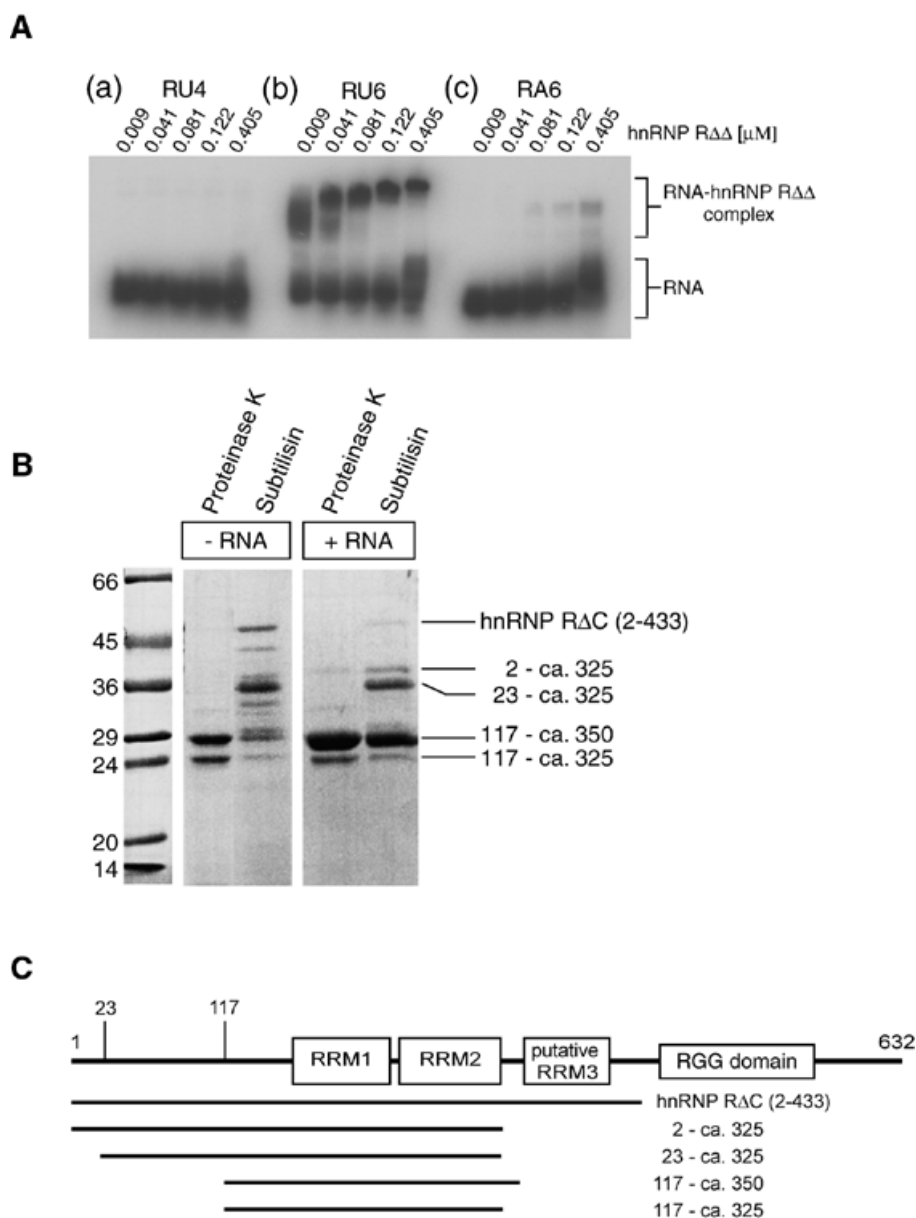


Figure 6. hnRNP-R binding to RNA. (A) Binding of hnRNP-R $\Delta\Delta$ (amino acids 26–433) to RNA was analysed by electrophoretic mobility shift. The strongest interaction was observed for an oligonucleotide with six terminal U nucleotides (b), whereas six adenosine (c) or four uridine nucleotides (a) interacted less intensely. A double band marks the shifted RNA possibly indicating multiple oligomerization states for the RNA-bound protein. (B) Limited proteolysis of hnRNP-R Δ C (amino acids 1–433) with proteinase K and subtilisin in the presence or absence of RNA. The position of molecular size standards is shown on the left, the fragment composition as determined by amino acid sequencing at the right side. (C) Diagram showing the position of the RRM motifs and the fragment composition after limited proteolysis in the presence or absence of RNA.

degeneration of motor neurons. Among other possibilities, Smn could exert motor neuron-specific activities in addition to its reported role in splicing and transcriptional regulation, that are not important for the function of other cells. These activities may be attributable to the Smn protein itself or to differences in the interaction with other partners that play functionally important roles in motor neurons. Interestingly, Smn is not only located in nuclear structures of motor neurons but also in the cytoplasm, in particular in axons (10,44,46). Therefore, we focussed on the identification of novel binding partners that co-localize with Smn in the axon of spinal motor neurons.

We describe two members of the hnRNP protein family as novel binding partners of SMN. hnRNP-R and hnRNP-Q interact with Smn both in Y2H screens and in co-immunoprecipitation. This interaction is only detectable with wild-type, full-length Smn protein but not with mutated Smn isoforms corresponding to human mutations E134K, S262I, T274I, Y272C, G279V, Δ exon7, Δ exon5, Δ exon5 and 7 (3,38–43) or Smn isoforms lacking regions encoded by exon 5 and/or 7. Thus, hnRNP-R and hnRNP-Q resemble other Smn binding partners such as the Sm proteins or RHA (7,22,24,47), which also do not bind to mutated or truncated Smn isoforms.

We also found that hnRNP-R interacts with RNA with a preference for poly(U) stretches. This result is complemented by the observation that hnRNP-R is present as a monomer in solution but upon binding of RNA forms oligomers, most probably dimers. Additional evidence comes from limited proteolysis in the presence or absence of RNA. RNA binding leads to enhanced protection of the N-terminal RRM domains which previously have been described as RNA interaction motifs (reviewed in 48). The C-terminal part of both hnRNP-R and hnRNP-Q contains an arginine-glycine-rich region resembling the RGG motifs in other Smn-binding proteins (27). This domain most probably mediates the interaction with Smn. It will be interesting to see whether post-translational methylation of arginines is required for high-affinity binding to Smn as shown for SmD1 and SmD3 (49).

As a first step into the physiological characterization of hnRNP-R and hnRNP-Q we tested their developmental and tissue-specific expression. Both proteins are widely expressed, both on the mRNA and protein level. Highest expression levels of hnRNP-R and hnRNP-Q during development of the spinal cord can be found during late embryogenesis around E19. Interestingly, the reduction of hnRNP-R and hnRNP-Q protein levels after birth apparently is due to post-transcriptional and/or post-translational mechanisms, as previously observed for SIP1/Gemin2. This suggests that the interaction with Smn controls the stability of interacting proteins. hnRNP-R co-localizes with Smn in the cytoplasm of the motor neurons including the axons. It is also found in the nucleus but not concentrated in gems. Thus, it is unlikely that hnRNP-R participates in specific functions of Smn complexes such as pre-mRNA splicing and regeneration of spliceosomal complexes (7). hnRNP-R was detectable in the cytoplasm and in axons of motor neurons as revealed by co-staining with PC1C6 anti-phospho-tau-1 antibodies. Staining of various peripheral nerves confirmed the presence of relatively high levels of hnRNP-R in motor axons.

hnRNP-Q has originally been identified as a glycine-arginine-tyrosine-rich putative RNA-binding protein (50) (gry-rbp; accession no. AF093821). It appears as an alternatively spliced version of NSAP1 (NS1-associated protein 1), which was identified as an interaction partner of a multifunctional protein required for viral replication of the minute virus of mice (33). In addition, NSAP1 has been implicated in the regulation of specific mRNA transport (33). hnRNP-Q/gry-rbp has been found in protein complexes involved in translationally coupled mRNA turnover (51) and mRNA splicing (32). hnRNP-Q has recently been described as an SMN-interacting protein. Depletion of hnRNP-Q from HeLa nuclear extracts was found to inhibit splicing of candidate pre-mRNAs. Thus, the interaction of SMN and hnRNP-Q could also play a role in pre-mRNA splicing (36). An alternatively spliced isoform of hnRNP-Q has also been described as the synaptotagmin-binding protein SYNCRIP with a putative role in organelle-based mRNA transport along the cytoskeleton (synaptotagmin-binding, cytoplasmic RNA-interacting protein) (34). These shorter isoforms of hnRNP-Q lack the glutamine- and asparagine-rich C-terminus present in full-length hnRNP-R and hnRNP-Q. Recently, hnRNP-Q protein has been shown to be a component of the apobec-1 editosome (35,50). All of these data point to the direction that hnRNP-R and hnRNP-Q specifically bind mRNAs, are involved in mRNA processing including editing, in mRNA transport and

finally act as regulators which modify binding to ribosomes and RNA translation. Such functions appear highly important for neurons with long processes, in particular motor neurons in which specific mRNAs have to be transported over long distances. The length of motor axons can exceed the diameter of the cell body by a factor of more than 5000, thus underlining the relevance of control mechanisms for mRNA transport to distant cellular sites such as to growth-cones or motor endplates (52,53). Indeed, Smn and hnRNP-R are concentrated and co-localized in the distal axon of isolated embryonic motor neurons.

This finding is also in accordance with observations, that the Smn protein is found independently from SIP1/Gemin2 in motor axons (44). At the electron microscopic level, it could be demonstrated that Smn immunoreactivity is associated with microtubules in motor axons during post-natal development (46). Thus, a complex of SMN and hnRNP-Q/SYNCRIP could modulate mRNA transport along microtubuli (34).

Further investigations on the functional relationship between Smn and hnRNPs may help to solve the question why motor neurons are exceptionally vulnerable to reduced levels of ubiquitously expressed SMN. Ultimately, this could lead to a better understanding of the mechanisms which lead to axonal degeneration and finally to motor neuron cell death in SMA.

MATERIALS AND METHODS

Yeast two-hybrid screen

A Y2H screen was performed using cDNA encoding murine *Smn* exon 2b–7 as a bait. Exon 1 was deleted in order to select against SIP1/Gemin2 which strongly interacts with the N-terminal of the SMN protein. The cDNA corresponding to exon 2b–7 was cloned into the plasmid pAS2-1 (Clontech) in-frame with the DNA-binding domain of *GAL4* by linker PCR (Smn2bBH1up, TTA TGG ATC CAT GCT CTA AAG AAC GGT GAC ATT TG and SmnBH1low, AGA AGG ATC CCC ATC TCC TGA GAC AGA GCT G). The screen was performed in the yeast strains CG1945 and Y190 (Clontech) using the 'HIS3 jump start' protocol according to the manufacturer's instructions. Briefly, after transformation of bait and library, cells were plated on SC-Trp-Leu medium at high density, selecting just for the presence of both proteins. Afterwards, yeast colonies were scratched from the plates and plated on SC-His-Trp-Leu + 5 mM 3AT to select for the expression of the *HIS3* reporter gene. Inserts were amplified from freshly grown colonies by PCR. Positive clones were sorted into groups with identical insert according to the restriction pattern with *HaeIII*. Representatives of these groups were purified and co-transformed into yeast with the original *Smn* bait to verify specific activation of the *HIS3* and *lacZ* reporter genes.

Generation of polyclonal antibodies against hnRNP-R and hnRNP-Q

Two rabbits were immunized with peptides specific for hnRNP-R or hnRNP-Q (hnRNP-R amino acids 1–18, MANQVNGNAVQLKEEEEP, and hnRNP-Q amino acids 1–18, MATEHVNGNGTEEPMDTT) in complete (first immunization) and incomplete (boost injections) Freund's adjuvans. The sequence of the peptides used for raising antisera is identical to

the human sequence of hnRNP-R and hnRNP-Q. Ten days after boost injections, blood was taken from the ear, serum prepared and the antisera analysed by western blot.

Cloning of mutated *Smn* cDNAs and hnRNP-R and hnRNP-Q cDNAs for co-immunoprecipitation

A series of mutations within the *SMN* gene have been identified in SMA patients, in particular within the C-terminal domain and the tudor domain of *Smn* (E134K, S262I, T274I, Y272C, G279V, Δ exon7, Δ exon5, Δ exon5 and 7 (3,38–43), thus interfering with the function(s) of *Smn*. We have generated constructs harbouring the corresponding mutations in the murine *Smn* cDNA sequence. Deletions and point mutations were introduced into the mouse *Smn* gene by using the PCR-based splicing by overlap extension method with different mismatch primers: *Smn* 5', GGA AGC TTA TGA TAA AGC TGT GGC TTC; *Smn* 3', CGC GGA TCC TTT TAT TTA ATT CTA AAG GCA TTA ATA AAA ATC TTG; Ex6msmnf272, GAG TGG CTG CCA CAC TGG CTA C; Ex6msmnr272, AGT AGC CAG TGT GGC AGC CAC TC; Ex6/8msmnf, CCA CAC TGG CTA CTA TAT GGT TCA GCT CTG TCT CAG G; Ex6/8msmnr, CCT GAG ACA GAG CTG AAC CAT ATA GTA GCC AGT GTG; E134Kf, GGA TAT GGA AAC AGA AAG GAG CAA AAC TT; E134Kr, AAG TTT TGC TCC TTT CTG TTT CCA TAT CC; s262if, TAG CAT AAT GCC CAG GGC ATC; s262ir, GAT GCC CTG GGC ATT ATG CT; t274if, GAG TGG CTA CCA CAT TGG CTA C; t274ir, AGT AGC CAG TGT GGC AGC CAC TC; Ex7msmnf279, GGC TAC TAT ATG GGT TTC AG; Ex7msmnr279, CTG AAA ACC ATA TAG TAG CC; Ex4/6msmnf, AGG ATT AGG ACC AGG AAA GAT AAT CCC GCC ACC CCC TCC; Ex4/6msmnr, AGG GGG TGG CGG GAT TAT CTT TCC TGG TCC TAA TCC TG.

For this purpose, the cDNA corresponding to a fragment composed of exon 2b–7 was ligated into a *Hind*III and *Bam*HI site of the pBluescript vector. The cDNA was used as template for further PCR amplifications. The resulting cDNA and expression vectors were subjected to automated DNA sequencing to confirm that the corresponding deletions/point mutations had been introduced and to exclude potential PCR artefacts.

Full-length cDNA of hnRNP-Q was obtained by using RT-PCR with mouse brain RNA with primers based on the published sequence of hnRNP-Q. In the case of hnRNP-R, the five-terminal sequence was established by RACE (5' RACE kit; Clontech). hnRNP-R and hnRNP-Q were amplified and cloned into pcDNA3 by linker PCR (hnrnpr-HA-up, AGA GGT ACC ACC ATG GGC TAC CCC TAC GAC GTG CCC; rnp-Xba-low, ATA TCT AGA CTA CTT CCA CTG CCC ATA AGT ATC; gry-rbp-HA-up, AGA GGT ACC ATG TAC CCC TAC GAC GTG CCC GAC TAC GCC ATG GCT ACA GAA CAT GTT; gry-Eco-low, ATA GAA TTC TAC TTC CAC TGC CCA AAA G). The full-length coding sequence of mouse hnRNP-R was deposited in GenBank with the accession no. AF441128.

Co-immunoprecipitations

Co-immunoprecipitations were carried out using 100 μ l antiserum pre-incubated with protein A- or G-agarose in lysis buffer (20 mM Tris pH 7.4, 137 mM NaCl, 10% glycerol, 1%

Triton X-100 2 mM EDTA, 50 mM Na- β -glycerophosphate, 20 mM Na-pyrophosphate, protease inhibitors). After three rounds of washing, the resulting suspensions were incubated with 100 μ g protein extract overnight at 4°C. The next day the co-immunoprecipitates were washed three times with lysis buffer and denatured in Laemmli buffer. Extracts were separated on a 10% polyacrylamide gel and transferred to nitro-cellulose membrane (Schleicher & Schuell). Blots were probed with monoclonal anti-*Smn* antibody or anti-FLAG antibody (Sigma).

Western blot analysis

Heart, liver, lung, kidney, spleen, muscle, brain and spinal cord from adult wild-type mice and spinal cord from different developmental stages were dissected from wild-type C57Bl/6 mice. The tissues were homogenized with RIPA buffer (50 mM Tris pH 7.5, 150 mM NaCl, 1% Nonidet P-40, 0.5% sodium deoxycholate, 0.1% SDS). After centrifugation, the protein concentration of the supernatants was determined using the Bio-Rad protein assay kit (Bio-Rad) according to the manufacturer's instructions. Each protein extract was mixed with the same volume of sample buffer (125 mM Tris pH 6.8, 4% SDS, 10% β -mercaptoethanol, 20% glycerol, 0.004% bromophenol blue). The samples were boiled for 2 min and stored at -20°C . Extracts were separated on a 10% polyacrylamide gel and transferred to a nitrocellulose membrane (Schleicher & Schuell). Unspecific binding sites on the membrane were blocked for 30 min with 5% instant milk powder in TBS containing 0.2% Tween (TBS-T). Primary antibodies including the monoclonal anti-mouse *Smn* IgG1 (250 μ g/ml; Dianova) and the polyclonal rabbit antiserum directed against hnRNP-R and hnRNP-Q were diluted 1:1000 in 5% instant milk powder in TBS-T. The antibodies were incubated with the membrane for 1 h at room temperature (RT). The membrane was washed three times for 15 min at RT with TBS-T. Goat anti-mouse and goat anti-rabbit HRP-conjugated antibodies (Roche) were used as secondary antibodies at a dilution of 1:10 000 with 5% instant milk in TBS-T. The membrane was incubated for 1 h at RT and subsequently washed three times. Then, the *Smn* immunoreactive bands were visualized using ECL chemiluminescent reagent (Amersham) according to the manufacturer's instructions. The blots were exposed to X-ray film for the detection of the chemiluminescent emissions. Each experiment was repeated at least twice. Stripping and reprobing of the blots was performed according to the manufacturer's protocols.

RT-PCR

Heart, liver, lung, kidney, spleen, muscle, brain and spinal cord from adult wild-type mice and spinal cord from different developmental stages of wild-type mice were dissected. RNA was prepared using the TRIZOL method (Life Technologies). PCR was performed using the following primer pairs: β -actin-s, GTG GGC CGC CCT AGG CAC CAG; β -actin-as, CTC TTT AAT GTC ACG CAC GAT TTC; RNP1F, ATG GCT AAT CAG GTG AAT GGT AAT G; RNP282R, AGTA CAG ACA GAG TCC CTT CCT C; gry1F, ATG GCT ACA GAA CAT GTT AAT GG; gry273R, AGC ACT GCC AAT GCG CCG TCT TC.

Immunodetection of Smn, hnRNP-R and tau in spinal motor neurons from spinal cord sections

The lumbar spinal cord from 12-month-old C57Bl/6 mice was dissected, and the L4 segment identified and frozen in Tissuetec (Sakura). Frozen sections (10 μ m) were prepared, blocked with TBS-T containing 10% BSA for 20 min at RT, and incubated with a monoclonal antibody against mouse Smn at 1 μ g/ml or a monoclonal antibody against phosphorylated tau-1 (clone PC1C6; Boehringer Mannheim) at 10 μ g/ml and polyclonal antibodies against hnRNP-R (1:1000). The samples were washed three times with TBS-T, incubated with secondary antibodies [Cy3TM-conjugated goat anti-rabbit IgG (Dianova) and Alexa-conjugated anti-mouse IgG (Roche Molecular Biochemicals)], washed again three times with TBS-T, embedded with DABCO (Merck) and covered with glass slides. Smn and hnRNP-R immunoreactivity was visualized with a Leica confocal microscope. The settings for pinhole and voltage were identical for the analysis of all sections. Experiments were repeated at least two times, data shown are from one representative experiment.

Techniques for embryonic motor neuron cell culture

Pregnant mice (14 days after conception) were killed by cervical dislocation, embryos dissected from the uterus and decapitated prior to further handling. Cultures of spinal motor neurons from E14 mice were prepared by panning with antibodies against the mouse p75 neurotrophin receptors (54) which is highly expressed only on developing motor neurons within the spinal cord. The ventrolateral part of the lumbar spinal cord was dissected and transferred to HBSS containing 10 μ M 2-mercaptoethanol. After treatment with trypsin (0.05%, 10 min), tissues were triturated and the cell suspension passed through a nylon mesh (100 μ m pore size). Cells were plated at a density of 3000 cells/cm² in four-well culture dishes (Greiner), precoated with poly-ornithine and laminin as described by Wiese *et al.* (54). Cells were grown in neurobasal medium (Life Technologies) with serum, 500 μ M glutamax and 50 μ g/ml apotransferrin at 37°C in a 5% CO₂ atmosphere. Fifty percent of the medium was replaced at day 1 and then every second day.

Motor neurons kept in culture for 7 days were fixed with methanol/acetone (1:1), blocked and incubated with a mouse monoclonal antibody against Smn, phospho-tau at 1 μ g/ml and/or polyclonal hnRNP-R antiserum (1:1000), washed three times with TBS-T, incubated with secondary antibodies (Cy3TM-conjugated goat anti rabbit IgG and Alexa-conjugated mouse IgG) washed again three times with TBS-T, and embedded in Mowiol. Immunoreactivity was visualized with a Leica confocal microscope, with identical settings for pinhole and voltage for any panel of analysis of motor neurons.

Overexpression and purification of hnRNP-R and hnRNP-R domains

The cDNAs coding for full-length hnRNP-R and the fragments hnRNP-R Δ N (amino acids 26–632), hnRNP-R Δ C (amino acids 1–433), and hnRNP-R $\Delta\Delta$ (amino acids 26–433) were amplified by PCR (primers: R_full, GGA ATT CC ATA TGG CTA ATC AGG TG; R_deltaN, GGA ATT CCA TAT GCA CAC AGA ACA CTA C; R_full_rev, CGG AAT TCT TAC

TAC TTC CAC TGT TGC; R_deltaC_rev, CGG AAT TCT TAA TCT TCA TAC GCA GTG C). The primers contained restriction enzyme recognition sites for cloning into the pET22b(+) (Novagen) expression vector. hnRNP-R Δ C and hnRNP-R $\Delta\Delta$ were expressed in *E.coli* BL21 (DE3) in LB medium + 200 mg/ml ampicillin at 37°C. Expression was induced by adding 1 mM IPTG at an OD₆₀₀ of 0.8. Cells were harvested 4 h after induction by centrifugation (30 min, 4200 r.p.m., Beckmann JS4.2 rotor, 6°C) and resuspended in 50 mM MOPS, pH 7.0, 100 mM NaCl, 1 mM EDTA, 2 mM MgCl₂, 2.5 mM DTT. Cells were disrupted by sonication and the lysate was cleared by centrifugation (35 min, 30 000 g, 4°C). The supernatant was filtered through a 2 μ m filter and loaded onto a Resource Q anion exchange column (Amersham Pharmacia Biotech) on an Äkta FPLC system (Amersham Pharmacia Biotech). The column was washed with buffer A [25 mM Tris-HCl pH 8.0, 0.1 NaCl, 3 mM MgCl₂, 0.1 mM EDTA, 0.5 mM DTT and 9% (v/v) glycerol], and the flow through fraction was loaded onto a 5 ml Heparin Hitrap column (Amersham Pharmacia Biotech). The protein was eluted with 50 ml buffer A with a linear gradient from 0.1 to 1 M NaCl. Fractions containing the recombinant protein were pooled, loaded on a 10 ml poly(U)-Sepharose affinity column (Amersham Pharmacia Biotech), and eluted over four column volumes with the same gradient. The fractions containing pure protein as judged from Coomassie blue-stained SDS-PAGE were concentrated in Centricon 10K (Millipore) to 10 mg/ml and the buffer exchanged to buffer B (10 mM Tris-HCl pH 7.5, 10 mM NaCl, 3 mM MgCl₂). The protein was re-concentrated to 13 mg/ml, shock-frozen in liquid nitrogen and stored at -20°C. Protein concentrations were determined by absorption at 280 nm by using the calculated extinction coefficient 33 950 M⁻¹ cm⁻¹ for hnRNP-R $\Delta\Delta$ and hnRNP-R Δ C.

Limited proteolysis and N-terminal microsequencing

A 9 μ g aliquot of hnRNP-R Δ C in 14.2 μ l buffer B was supplemented with 0.8 μ l proteinase K or subtilisin (0.1 mg/ml in buffer B, respectively). After 30 min incubation at 25°C, digestion was stopped by addition of 15 μ l hot Laemmli SDS-PAGE sample buffer and immediate boiling for 5 min. Samples were analysed by SDS-PAGE [12% (w/v) acrylamide] and staining with Coomassie blue. Samples used for N-terminal microsequencing were electro-blotted to PVDF membrane, and the sequencing of individual bands was carried out by Dr K.-H.Mann (Max-Planck-Institut für Biochemie, Martinsried, Germany).

Electrophoretic mobility shift assay

The RNA oligomers RU6, 5'-GGCUUUUUU-3', RU4 5'-GGCUUUU-3' and RA6 5'-CCGAAAAA-3', were synthesized by Dr Arnold (Ludwig-Maximilian-Universität, Munich, Germany). The RNA oligonucleotides RU6, RU4 and RA6 were labelled at the 5' end with T4 polynucleotide kinase and [γ -³²P]dATP (Amersham Pharmacia Biotech) and purified on G25 spin columns (Amersham Pharmacia Biotech). 10 000 c.p.m. of these substrates (~900 ng) was mixed with 0.01–0.5 μ M hnRNP-R $\Delta\Delta$ in 25 mM Tris-HCl pH 8.0, 100 mM NaCl, 3 mM MgCl₂, 0.1 mM EDTA, 0.5 mM DTT and 0.5% Nonidet P-40. The samples were incubated on ice for 30 min in a total volume of 22 μ l, and upon addition of loading dye [40%

sucrose, 0.01% (w/v) xylene cyanol], the samples were resolved at 4°C on a pre-run 9% native polyacrylamide gel in 0.5× TBA (34 mM Tris, 45 mM boric acid, 0.1 mM EDTA). Gels were run at 110 V for 1 h, vacuum dried onto Whatman 3MM paper and exposed to X-ray film. Quantitation of radioactively labelled RNA probes was done on a Fuji PhosphorImager system.

ACKNOWLEDGEMENTS

We thank Jennifer Kara and Stefanie Renninger for great technical assistance and Stefan Wiese for expert advice in motor neuron culture. This work was supported by grants for SFB 581, TPB1, TPB4 and SFB 465, TPA3.

REFERENCES

- Korinthenberg, R., Sauer, M., Ketelsen, U.P., Hanemann, C.O., Stoll, G., Graf, M., Baborie, A., Volk, B., Wirth, B., Rudnik-Schoneborn, S. and Zerres, K. (1997) Congenital axonal neuropathy caused by deletions in the spinal muscular atrophy region. *Ann. Neurol.*, **42**, 364–368.
- Melki, J. (1997) Spinal muscular atrophy. *Curr. Opin. Neurol.*, **10**, 381–385.
- Lefebvre, S., Burglen, L., Rebollet, S., Clermont, O., Burlet, P., Viollet, L., Benichou, B., Cruaud, C., Millasseau, P., Zeviani, M. *et al.* (1995) Identification and characterization of a spinal muscular atrophy-determining gene. *Cell*, **80**, 155–165.
- Wirth, B. (2000) An update of the mutation spectrum of the survival motor neuron gene (SMN1) in autosomal recessive spinal muscular atrophy (SMA). *Hum. Mutat.*, **15**, 228–237.
- Lorson, C.L. and Androphy, E.J. (2000) An exonic enhancer is required for inclusion of an essential exon in the SMA-determining gene SMN. *Hum. Mol. Genet.*, **9**, 259–265.
- Lefebvre, S., Burlet, P., Liu, Q., Bertrand, S., Clermont, O., Munnich, A., Dreyfuss, G. and Melki, J. (1997) Correlation between severity and SMN protein level in spinal muscular atrophy. *Nat. Genet.*, **16**, 265–269.
- Pellizzoni, L., Charroux, B. and Dreyfuss, G. (1999) SMN mutants of spinal muscular atrophy patients are defective in binding to snRNP proteins. *Proc. Natl Acad. Sci. USA*, **96**, 11167–11172.
- Pellizzoni, L., Kataoka, N., Charroux, B. and Dreyfuss, G. (1998) A novel function for SMN, the spinal muscular atrophy disease gene product, in pre-mRNA splicing. *Cell*, **95**, 615–624.
- Covert, D.D., Le, T.T., McAndrew, P.E., Strasswimmer, J., Crawford, T.O., Mendell, J.R., Coulson, S.E., Androphy, E.J., Prior, T.W. and Burghes, A.H. (1997) The survival motor neuron protein in spinal muscular atrophy. *Hum. Mol. Genet.*, **6**, 1205–1214.
- Jablonka, S., Schrank, B., Krawski, M., Rossoll, W. and Sendtner, M. (2000) Reduced survival motor neuron (Smn) gene dose in mice leads to motor neuron degeneration: an animal model for spinal muscular atrophy type III. *Hum. Mol. Genet.*, **9**, 341–346.
- Frugier, T., Tiziano, F.D., Cifuentes-Diaz, C., Miniou, P., Roblot, N., Dierich, A., Le Meur, M. and Melki, J. (2000) Nuclear targeting defect of SMN lacking the C-terminus in a mouse model of spinal muscular atrophy. *Hum. Mol. Genet.*, **9**, 849–858.
- Monani, U.R., Sendtner, M., Covert, D.D., Parsons, D.W., Andreassi, C., Le, T.T., Jablonka, S., Schrank, B., Rossoll, W., Prior, T.W., Morris, G.E. and Burghes, A.H. (2000) The human centromeric survival motor neuron gene (SMN2) rescues embryonic lethality in *Smn*^{-/-} mice and results in a mouse with spinal muscular atrophy. *Hum. Mol. Genet.*, **9**, 333–339.
- Hsieh-Li, H.M., Chang, J.G., Jong, Y.J., Wu, M.H., Wang, N.M., Tsai, C.H. and Li, H. (2000) A mouse model for spinal muscular atrophy. *Nat. Genet.*, **24**, 66–70.
- Schrank, B., Gotz, R., Gunnarsen, J.M., Ure, J.M., Toyka, K.V., Smith, A.G. and Sendtner, M. (1997) Inactivation of the survival motor neuron gene, a candidate gene for human spinal muscular atrophy, leads to massive cell death in early mouse embryos. *Proc. Natl Acad. Sci. USA*, **94**, 9920–9925.
- Liu, Q. and Dreyfuss, G. (1996) A novel nuclear structure containing the survival of motor neurons protein. *EMBO J.*, **15**, 3555–3565.
- Fischer, U., Liu, Q. and Dreyfuss, G. (1997) The SMN–SIP1 complex has an essential role in spliceosomal snRNP biogenesis. *Cell*, **90**, 1023–1029.
- Charroux, B., Pellizzoni, L., Perkinson, R.A., Shevchenko, A., Mann, M. and Dreyfuss, G. (1999) Gemin3: A novel DEAD box protein that interacts with SMN, the spinal muscular atrophy gene product, and is a component of gems. *J. Cell Biol.*, **147**, 1181–1194.
- Charroux, B., Pellizzoni, L., Perkinson, R.A., Yong, J., Shevchenko, A., Mann, M. and Dreyfuss, G. (2000) Gemin4. A novel component of the SMN complex that is found in both gems and nucleoli. *J. Cell Biol.*, **148**, 1177–1186.
- Campbell, L., Hunter, K.M., Mohaghegh, P., Tinsley, J.M., Brasch, M.A. and Davies, K.E. (2000) Direct interaction of Smn with dp103, a putative RNA helicase: a role for Smn in transcription regulation? *Hum. Mol. Genet.*, **9**, 1093–1100.
- Meister, G., Buhler, D., Lagerbauer, B., Zobawa, M., Lottspeich, F. and Fischer, U. (2000) Characterization of a nuclear 20S complex containing the survival of motor neurons (SMN) protein and a specific subset of spliceosomal Sm proteins. *Hum. Mol. Genet.*, **9**, 1977–1986.
- Giesemann, T., Rathke-Hartlieb, S., Rothkegel, M., Bartsch, J.W., Buchmeier, S., Jockusch, B.M. and Jockusch, H. A role for polyproline motifs in the spinal muscular atrophy protein SMN. Profilins bind to and colocalize with smn in nuclear gems. *J. Biol. Chem.*, **274**, 37908–37914.
- Buhler, D., Raker, V., Luhrmann, R. and Fischer, U. (1999) Essential role for the tudor domain of SMN in spliceosomal U snRNP assembly: implications for spinal muscular atrophy. *Hum. Mol. Genet.*, **8**, 2351–2357.
- Selenko, P., Sprangers, R., Stier, G., Buhler, D., Fischer, U. and Sattler, M. (2001) SMN tudor domain structure and its interaction with the Sm proteins. *Nat. Struct. Biol.*, **8**, 27–31.
- Pellizzoni, L., Charroux, B., Rappalber, J., Mann, M. and Dreyfuss, G. (2001) A functional interaction between the survival motor neuron complex and RNA polymerase II. *J. Cell Biol.*, **152**, 75–85.
- Pellizzoni, L., Baccon, J., Charroux, B. and Dreyfuss, G. (2001) The survival of motor neurons (SMN) protein interacts with the snRNP proteins fibrillarin and GAR1. *Curr. Biol.*, **11**, 1079–1088.
- Jones, K.W., Gorzynski, K., Hales, C.M., Fischer, U., Badbanchi, F., Terns, R.M. and Terns, M.P. (2001) Direct interaction of the spinal muscular atrophy disease protein SMN with the small nucleolar RNA-associated protein fibrillarin. *J. Biol. Chem.*, **276**, 38645–38651.
- Friesen, W.J. and Dreyfuss, G. (2000) Specific sequences of the Sm and Sm-like (Lsm) proteins mediate their interaction with the spinal muscular atrophy disease gene product (SMN). *J. Biol. Chem.*, **275**, 26370–26375.
- Grohmann, K., Schuelke, M., Diers, A., Hoffmann, K., Lucke, B., Adams, C., Bertini, E., Leonhardt-Horti, H., Muntoni, F., Ouvrier, R. *et al.* (2001) Mutations in the gene encoding immunoglobulin μ -binding protein 2 cause spinal muscular atrophy with respiratory distress type 1. *Nat. Genet.*, **29**, 75–77.
- Strasswimmer, J., Lorson, C.L., Breiding, D.E., Chen, J.J., Le, T., Burghes, A.H. and Androphy, E.J. (1999) Identification of survival motor neuron as a transcriptional activator-binding protein. *Hum. Mol. Genet.*, **8**, 1219–1226.
- Grundhoff, A.T., Kremmer, E., Tureci, O., Glieden, A., Gindorf, C., Atz, J., Mueller-Lantzsch, N., Schubach, W.H. and Grasser, F.A. (1999) Characterization of DP103, a novel DEAD box protein that binds to the Epstein-Barr virus nuclear proteins EBNA2 and EBNA3C. *J. Biol. Chem.*, **274**, 19136–19144.
- Tucker, K.E., Berciano, M.T., Jacobs, E.Y., LePage, D.F., Shpargel, K.B., Rossire, J.J., Chan, E.K., Lafarga, M., Conlon, R.A. and Matera, A.G. (2001) Residual Cajal bodies in coilin knockout mice fail to recruit Sm snRNPs and SMN, the spinal muscular atrophy gene product. *J. Cell Biol.*, **154**, 293–307.
- Neubauer, G., King, A., Rappalber, J., Calvio, C., Watson, M., Ajuh, P., Sleeman, J., Lamond, A. and Mann, M. (1998) Mass spectrometry and EST-database searching allows characterization of the multi-protein spliceosome complex. *Nat. Genet.*, **20**, 46–50.
- Harris, C.E., Boden, R.A. and Astell, C.R. (1999) A novel heterogeneous nuclear ribonucleoprotein-like protein interacts with NS1 of the minute virus of mice. *J. Virol.*, **73**, 72–80.
- Mizutani, A., Fukuda, M., Ibata, K., Shiraishi, Y. and Mikoshiba, K. (2000) SYNCRIP, a cytoplasmic counterpart of heterogeneous nuclear ribonucleoprotein R, interacts with ubiquitous synaptotagmin isoforms. *J. Biol. Chem.*, **275**, 9823–9831.
- Lau, P.P., Chang, B.H. and Chan, L. (2001) Two-hybrid cloning identifies an RNA-binding protein, GRY-RBP, as a component of apobec-1 editosome. *Biochem. Biophys. Res. Commun.*, **282**, 977–983.

36. Mourelatos,Z., Abel,L., Yong,J., Kataoka,N. and Dreyfuss,G. (2001) SMN interacts with a novel family of hnRNP and spliceosomal proteins. *EMBO J.*, **20**, 5443–5452.
37. Hassfeld,W., Chan,E.K., Mathison,D.A., Portman,D., Dreyfuss,G., Steiner,G. and Tan,E.M. (1998) Molecular definition of heterogeneous nuclear ribonucleoprotein R (hnRNP R) using autoimmune antibody: immunological relationship with hnRNP P. *Nucleic Acids Res.*, **26**, 439–445.
38. Rodrigues,N.R., Owen,N., Talbot,K., Ignatius,J., Dubowitz,V. and Davies,K.E. (1995) Deletions in the survival motor neuron gene on 5q13 in autosomal recessive spinal muscular atrophy. *Hum. Mol. Genet.*, **4**, 631–634.
39. Hahnen,E., Schonling,J., Rudnik-Schoneborn,S., Raschke,H., Zerres,K. and Wirth,B. (1997) Missense mutations in exon 6 of the survival motor neuron gene in patients with spinal muscular atrophy (SMA). *Hum. Mol. Genet.*, **6**, 821–825.
40. Talbot,K., Rodrigues,N.R., Ignatius,J., Muntoni,F. and Davies,K.E. (1997) Gene conversion at the SMN locus in autosomal recessive spinal muscular atrophy does not predict a mild phenotype. *Neuromuscul. Disord.*, **7**, 198–201.
41. Bussaglia,E., Clermont,O., Tizzano,E., Lefebvre,S., Burglen,L., Cruaud,C., Urtizberea,J.A., Colomer,J., Munnich,A. and Baiget,M. (1995) A frame-shift deletion in the survival motor neuron gene in Spanish spinal muscular atrophy patients. *Nat. Genet.*, **11**, 335–337.
42. DiDonato,C.J., Ingraham,S.E., Mendell,J.R., Prior,T.W., Lenard,S., Moxley,R.T., Florence,J. and Burghes,A.H. (1997) Deletion and conversion in spinal muscular atrophy patients: is there a relationship to severity? *Ann. Neurol.*, **41**, 230–237.
43. Wirth,B., Herz,M., Wetter,A., Moskau,S., Hahnen,E., Rudnik-Schoneborn,S., Wienker,T. and Zerres,K. Quantitative analysis of survival motor neuron copies: identification of subtle SMN1 mutations in patients with spinal muscular atrophy, genotype–phenotype correlation, and implications for genetic counseling. *Am. J. Hum. Genet.*, **64**, 1340–1356.
44. Jablonka,S., Bandilla,M., Wiese,S., Buhler,D., Wirth,B., Sendtner,M. and Fischer,U. (2001) Co-regulation of survival of motor neuron (SMN) protein and its interactor SIP1 during development and in spinal muscular atrophy. *Hum. Mol. Genet.*, **10**, 497–505.
45. Wang,J. and Dreyfuss,G. (2001) A cell system with targeted disruption of the SMN gene: functional conservation of the SMN protein and dependence of Gemin2 on SMN. *J. Biol. Chem.*, **276**, 9599–9605.
46. Pagliardini,S., Giavazzi,A., Setola,V., Lizier,C., Di Luca,M., DeBiasi,S. and Battaglia,G. (2000) Subcellular localization and axonal transport of the survival motor neuron (SMN) protein in the developing rat spinal cord. *Hum. Mol. Genet.*, **9**, 47–56.
47. Lorson,C.L., Strasswimmer,J., Yao,J.M., Baleja,J.D., Hahnen,E., Wirth,B., Le,T., Burghes,A.H. and Androphy,E.J. SMN oligomerization defect correlates with spinal muscular atrophy severity. *Nat. Genet.*, **19**, 63–66.
48. Shamoo,Y., Abdul-Manan,N. and Williams,K.R. (1995) Multiple RNA binding domains (RBDs) just don't add up. *Nucleic Acids Res.*, **23**, 725–728.
49. Friesen,W.J., Massenet,S., Paushkin,S., Wyce,A. and Dreyfuss,G. (2001) SMN, the product of the spinal muscular atrophy gene, binds preferentially to dimethylarginine-containing protein targets. *Mol. Cell*, **7**, 1111–1117.
50. Blanc,V., Navaratnam,N., Henderson,J.O., Anant,S., Kennedy,S., Jarmuz,A., Scott,J. and Davidson,N.O. (2001) Identification of GRY-RBP as an apolipoprotein B RNA-binding protein that interacts with both apobec-1 and apobec-1 complementation factor to modulate C to U editing. *J. Biol. Chem.*, **276**, 10272–10283.
51. Grosset,C., Chen,C.Y., Xu,N., Sonenberg,N., Jacquemin-Sablon,H. and Shyu,A.B. (2000) A mechanism for translationally coupled mRNA turnover: interaction between the poly(A) tail and a c-fos RNA coding determinant via a protein complex. *Cell*, **103**, 29–40.
52. Mohr,E. and Richter,D. Axonal mRNAs: functional significance in vertebrates and invertebrates. *J. Neurocytol.*, **29**, 783–791.
53. Gallant,P.E. (2000) Axonal protein synthesis and transport. *J. Neurocytol.*, **29**, 779–782.
54. Wiese,S., Metzger,F., Holtmann,B. and Sendtner,M. (1999) The role of p75NTR in modulating neurotrophin survival effects in developing motoneurons. *Eur. J. Neurosci.*, **11**, 1668–1676.

